

# Quantification of land–sea nutrient fluxes supplied by allis shad across the species' range

Camille Poulet, Betsy L. Barber-O'Malley, Géraldine Lassalle, and Patrick Lambert

**Abstract:** Diadromous species act as nutrient vectors between their marine and freshwater habitats. Few valuations of this regulating service exist and none at the scale of species distribution ranges. This large-scale approach seems particularly relevant for species moving and exchanging individuals across borders and territories as these populations may strongly depend upon each other in terms of population viability and provision of ecosystem services. The development of a new nutrient routine within an existing mechanistic species distribution model provided estimates of the “maximum potential” of the anadromous allis shad (*Alosa alosa*) to provide nitrogen and phosphorous subsidies throughout western Europe. During their seasonal reproductive migration, shad provided low amounts of nutrient subsidies when compared to North American anadromous species and annual riverine nutrient loads. However, these subsidies are delivered as pulses concentrated in space and time, suggesting that more work is needed to figure out the significance of these shad-derived nutrients in terms of riverine ecosystem functioning. The evidence of a substantial flow of strays delivering nutrient subsidies in several rivers confirmed the need for large-scale management of migratory species to ensure a sustainable provision of ecosystem services.

**Résumé :** Les espèces diadromes agissent comme vecteurs de nutriments entre leurs habitats marins et d'eau douce. Il existe peu d'évaluations de ce service de régulation et aucune à l'échelle d'aires de répartition d'espèces. Cette approche à grande échelle semble particulièrement pertinente pour les espèces qui traversent des frontières et échangent des individus, puisque ces populations pourraient dépendre fortement les unes des autres en ce qui attrait à leur viabilité et à la fourniture de services écosystémiques. L'élaboration d'une nouvelle routine de traitement des nutriments dans un modèle mécaniste existant de répartition des espèces produit des estimations du « potentiel maximum » de l'alose (*Alosa alosa*), une espèce anadrome, à fournir de l'azote et du phosphore partout en Europe de l'Ouest. Durant leur migration de reproduction saisonnière, les aloses fournissent de petites quantités de nutriments comparativement à des espèces anadromes nord-américaines et aux charges annuelles de nutriments dans les rivières. Ces apports sont cependant livrés sous forme de pulses concentrés dans l'espace et le temps. Plus de travaux sont donc nécessaires pour établir l'importance de ces nutriments dérivés d'aloses pour le fonctionnement d'écosystèmes fluviaux. L'observation de flux considérables d'individus vagabonds qui fournissent ces nutriments dans plusieurs rivières confirme qu'une gestion à grande échelle est nécessaire pour les espèces migratrices afin d'assurer une prestation durable de services écosystémiques. [Traduit par la Rédaction]

## Introduction

Diadromous species (land–sea migrating fishes) are cross-border resources; they move between fresh and marine waters to complete their life cycles (McDowall 1988), and population exchange can occur among river basins in different territories and administrative boundaries. Given this complex life cycle, diadromous species have been adversely affected by multiple human activities (e.g., overexploitation, degradation of essential habitats, losses of connectivity, pollution, water withdrawal, climate change). These cumulative pressures led to a generalized decline in abundances across their distribution ranges with drastic losses of associated services provided to local human communities (Limburg and Waldman 2009; Wilson and Veneranta 2019). In terms of provisioning services, diadromous species have been targeted by commercial fisheries over centuries and across continents and are highly prized in aquaculture food production (Kobayashi et al. 2015). They were recognized as one of the major protein and bioavailable micronutrient sources for human communities across

the world (Hicks et al. 2019). For example, Salmonidae contain high percentages of fatty acids essential to human health (Joordens et al. 2014). Diadromous species also provide cultural services and are historically prevalent in cultural practices (e.g., brotherhoods and ceremonies), gastronomy, diet, medicines and material items (e.g., Bolster 2008). Some of these species are described as charismatic, emblematic, and iconic (i.e., cultural keystone species census; Garibaldi and Turner 2004). The relative importance of the cultural services associated with diadromous species is suspected to be growing over time in relation with the global rarefaction of fish populations (Drouineau et al. 2018). As an example, in Sweden, Haro (2009) reported a massive shift from commercial to recreational fisheries due to a declining trend in fish abundances. Consequently, recreational fishing has gradually become a high-value recreational activity across the Baltic region and elsewhere (Hyder et al. 2018).

Besides their well-known significance in terms of provisioning and cultural services, diadromous species have also been recog-

Received 19 January 2021. Accepted 5 July 2021.

C. Poulet, G. Lassalle, and P. Lambert. INRAE, UR EABX, 50 Avenue de Verdun, 33612 Cestas Cedex, France.

B.L. Barber-O'Malley.\* INRAE, UR EABX, 50 Avenue de Verdun, 33612 Cestas Cedex, France; University of Maine, 168 College Avenue, Orono, ME 04469, USA.

**Corresponding author:** Camille Poulet (email: [camille.poulet@inrae.fr](mailto:camille.poulet@inrae.fr)).

\*Present address: Gomez and Sullivan Engineers, 41 Liberty Hill Road, Henniker, NH 03242, USA.

© 2021 The Author(s). This work is licensed under a [Creative Commons Attribution 4.0 International License](https://creativecommons.org/licenses/by/4.0/) (CC BY 4.0), which permits unrestricted use, distribution, and reproduction in any medium, provided the original author(s) and source are credited.

nized as strong ecological drivers for major biological cycles because of their role as nutrient “conveyor belts”. In particular, anadromous species (which migrate from marine habitats to upstream rivers to spawn; McDowall 1988) accumulate substantial amounts of embodied marine nutrients during their growing phase at sea. These marine-derived nutrients are moved from the ocean into freshwater habitats through migrations and may positively affect estuarine and riverine ecosystem functioning. Of central significance are the semelparous anadromous species (fishes dying after reproduction). After spawning, decomposing carcasses provide a consistent and bioavailable source of nutrients for freshwater communities and food webs at multiple trophic levels (Samways et al. 2015, 2018; Twining et al. 2017). In particular, nutrient enrichment from carcasses increases the overall primary productivity (Durbin et al. 1979), the biomass of biofilm algae and fungi, the bacteria density (Samways et al. 2015) and modifies the macroinvertebrates assemblages at local scale (Guyette et al. 2014; Weaver et al. 2018). Increases in growth and survival of juveniles salmonids were also observed in streams receiving adult salmon subsidies, providing evidence for a positive feedback loop (Bilby et al. 1996; Wipfli et al. 2003; Scheuerell et al. 2005) with suspected evolutionary consequences at the species level (Auer et al. 2018).

Despite being a widely recognized process, quantitative estimates of these regulating services are still scarce, and mainly concern Pacific salmon (*Oncorhynchus* spp.) runs in North America. Pacific salmon-derived nutrients are released through the metabolism of spawning fish in the form of excretion and the decay of spawners' carcasses (Naiman et al. 2002; Schindler et al. 2003; Janetski et al. 2009). In the Columbia River, Gresh et al. (2000) estimated that Pacific salmon historically contributed over 3000 metric tons of nitrogen (N) and 360 metric tons of phosphorus (P) each year. Similarly to salmon from the US Pacific coast is the case of alosines (i.e., blueback herring (*Alosa aestivalis*) and alewife (*Alosa pseudoharengus*)) that used to provide large quantities of marine-derived nutrients throughout their native range along the US Atlantic coast (Durbin et al. 1979; Garman 1992; West et al. 2010). These previous works gave critical insights on the ecological roles of diadromous species in the nutrient status of river basins, particularly upper reaches. However, these studies were mostly catchment-specific and were only performed in a limited number of locations throughout the eastern US coast. Although migratory species produce and deliver ecosystem services locally, the dynamics of the species is often triggered by the spatial distribution of resources and thereby depend on habitats that are isolated spatially from the places where services are provided (Kremen et al. 2007). Thus, the supplies received by society from a migratory species are relying on favorable habitats encountered by the species in other parts of the range. On that, “spatial mismatches” are likely to occur between areas where species “provided the most ecosystem services” and those that “support population ability” to provide sustainable services (Semmens et al. 2011, 2018; MEA 2005). For diadromous species that migrate over long distances, “spatial mismatches” can occur within the same country, region, or states or far beyond political boundaries, leading to consider multiple spatial scales, from regional to inter-state, to find the most relevant one for conservation issues. Thus, having estimates of the nutrient subsidies translocated by shads at the scale of the distribution range in catchments for which no data were available is of particular relevance. Assessments and management of ecosystem services linked to diadromous species required consideration of larger spatial scales, and specific methods for estimating the extent to which distinct locations benefit or support the provision of ecosystem services between them. Such challenge requires an explicit consideration of fish movement and their magnitude, so that estimations of services explicitly including metapopulation dynamics and dispersal seem vital to address this management and conservation challenge (López-Hoffman et al. 2010).

In Europe, allis shad (*Alosa alosa*) populations have experienced a persistent and significant decline across their range (ICES 2015). Overfishing, water pollution, dam construction, habitat degradation, and more recently, invasive species can be held responsible for such a decrease (Limburg and Waldman 2009). In the Gironde–Garonne–Dordogne system (GGD) in France, known as the largest allis shad population in Europe, spawning runs of almost 400 000 fish migrating upstream in the 1980s have drastically declined to only thousands of fish at the end of the 20th century (Baglinière and Élie 2000; Castelnaud et al. 2001). Similar to the GGD, annual catches of shad in the Minho River (Spain–Portugal) decreased by about 90% after the 1950s (Mota et al. 2016). Therefore, the species was listed on the Red List of the International Union for the Conservation of Nature (IUCN 2020) and benefits from regional conservation status. Despite this overall decline, allis shad populations in “reference” basins in France, Spain, and Portugal are still considered of high cultural and ecological value, confirming the need for innovative scientific insights and perspectives to enhance management efforts at both local and global scales (see <https://diades.eu>).

In this context, the aim of this study was to provide the first quantification of nutrient imports and exports delivered by shad populations across its distribution range with explicit consideration of connections among different river basins. The case study of allis shad in Western Europe over the early 20th century was considered. A mechanistic species distribution model called G3RD (Global Repositioning Dynamics of Diadromous fish Distribution) was developed for any anadromous species and was first parameterized for allis shad (Rougier et al. 2014, 2015). The model was first used to assess the species range-shift response to the thermal component of climate change, suggesting that allis shad may be able to cope successfully with ongoing climate change that should not be perceived as a major threat to the species long-term persistence (Rougier et al. 2015). Integrating temperature was the most straightforward way to address the climate change issue on fish, given their ectothermic nature. Based on the existing literature, three life cycle processes (i.e., including growth at sea (Gilligan-Lunda et al. 2021), survival of spawners (Paumier et al. 2019), and survival of early life stages in rivers (Jatteau et al. 2017)) were linked to temperature to account for whole-life cycle impacts to global warming (Rougier et al. 2014). To assess the potential for shad to deliver nutrients across European river basins, an original nutrient routine providing estimates of nutrient imports and exports was designed and combined with GR3D. This study focused on evaluating the interdependences among river basins in the provision of nutrients subsidies in the context of metapopulation dynamics demonstrated for shad (Martin et al. 2015; Randon et al. 2018).

## Materials and methods

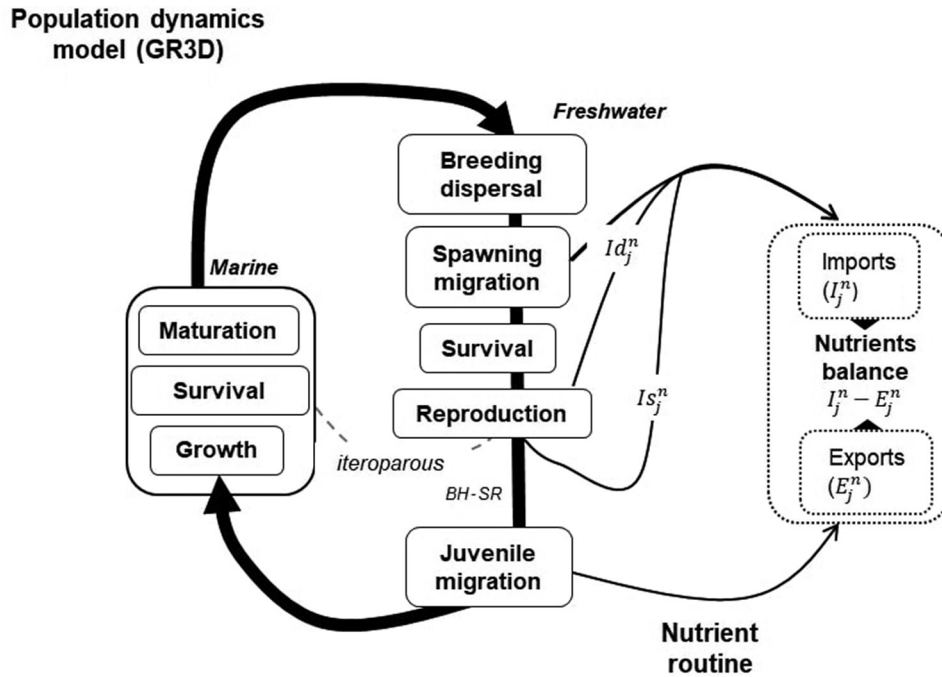
A brief description of the GR3D model and the key updates to improve and test the overall model robustness are provided in sections “GR3D model presentation and main improvements” and “Partial validation of estimated fish abundances”. The new routine added to GR3D to quantify nutrient fluxes is presented in the section “Design of the nutrient routine”. The updated code is available online at <https://github.com/inrae/GR3D/tree/v3.2.1> and <http://doi.org/10.5281/zenodo.4442030>. For a more detailed description of the GR3D model, see Appendix A or Rougier (2014) and Rougier et al. (2014).

### GR3D model presentation and main improvements

#### Population dynamics within the model

GR3D is an individual-based stochastic model. It explicitly combines population dynamics with key life cycle events and climatic requirements. The GR3D model was written in Java using the “SimAqualife” software framework specifically designed for

**Fig. 1.** Structure of the GR3D model after integration of the new nutrient routine. In the ocean, mature fish disperse in fresh water to spawn. The number of recruits produced is determined by a Beverton–Holt stock–recruitment curve (BH-SR). The nutrient balance is based on adult import derived from dead ( $I_d^n$ ) or living fish ( $I_s^n$ ) and out-migrating juvenile export. See Appendix A for a fully detailed description with model equations.



spatialized and individual-based simulations to explore the movements of aquatic species (Dumoulin 2007). The model covers the entire anadromous life cycle and is divided into six sub-models depicting the key events, including (i) reproduction, (ii) growth, (iii) survival, (iv) downstream migration, (v) maturation, and (vi) dispersal and upstream migration (Fig. 1). A set of 42 parameters obtained from the primary literature, expert elicitation, or model calibration was used to define these different processes. Most of the data used in GR3D came from the Garonne River in the south-west of France, which was considered as a “reference” population for shad in Europe (for more details, see Rougier et al. 2014, 2015) (Table A1 and Fig. A1). Three life cycle processes, including growth at sea, survival of spawner before they reproduce, and survival of early life stages in rivers, were linked to water temperature, as further described.

The “physical” environment of GR3D was divided into “two worlds”: the continental and marine compartments, which are split into a set of “river basins” and “sea basins”, respectively. River and sea basins are connected to each other and spatially geo-referenced. This “physical” environment represents the European Atlantic coast from the south of Portugal to the British Isles and Norway that covers the core distribution of the species (Fig. A1). River and sea basins are both characterized by seasonal temperature time series ( $T$ , °C), while river basins are also characterized by their surface area ( $\text{km}^2$ ) and geographic position (latitude and longitude at the river mouth).

Fish progressed through the life cycle with a seasonal time step. Reproduction occurred every spring in all rivers when spawners were present. The number of recruits produced by the spawning stock in river basin  $j$  was modeled as a density-dependent process using a Beverton and Holt stock–recruitment (BH-SR) relationship (Beverton and Holt 1957) (Fig. 1 and eq. A1). Egg production in basin  $j$  was linked to species fecundity ( $\alpha$ ) and the number of spawners present. The BH-SR relationship was modeled so that recruit mortality was dependent on both temperature and basin size to

consider resource limitations in small basins. The relationship between recruit mortality and temperature follows a dome-shaped curve (Rosso et al. 1995), with the number of recruits decreasing when temperature is below or above an optimal value. The tolerance and optimal thermal ranges are defined as model parameters (Table A1). An “Allee effect” (Stephens et al. 1999), proportional to the river basin size, was also integrated into the stock–recruitment relationship to prevent the formation of a functional population from only a limited number of individuals settling in a river basin.

In early summer, juveniles migrated from their upstream habitats through rivers and estuaries to reach the associated sea basin in the physical environment where they could grow and sexually mature. Fish growth was modeled using a von Bertalanffy growth function (von Bertalanffy 1938) (eq. A2). Since temperature is known to affect growth rate, a dome-shaped curve, similar to the one for reproduction, was used to link the growth coefficient ( $K$ , defined as a model parameter; Table A1) to water temperature and introduce seasonal and in-river variability on fish growth (Rosso et al. 1995; Kielbassa et al. 2010; Bal et al. 2011).

After spending several years at sea, ripe individuals started their spawning migration and entered a river basin to reproduce. An individual was assumed to be mature when it reached its size at maturity,  $L_{\text{mat}}$ , defined as a model parameter (Table A1).

Dispersal from the ocean to a given river basin occurred in three main steps: emigration, transfer, and settlement. Emigration depended on whether individuals adopted a homing behavior (i.e., individuals return to their natal river to reproduce) or a straying behavior (individuals colonize a new river basin that differs from their natal origin to reproduce). The probability of adopting a homing behavior ( $p_{\text{hom}}$ ) was considered as a specific life-history trait and hence did not vary among populations. Consequently, the probability of adopting a straying behavior ( $1 - p_{\text{hom}}$ ) was imposed to be the same for all rivers considered in this study. During the transfer phase, individuals adopting a homing behavior simply enter the natal river to spawn. For strayers, the

Can. J. Fish. Aquat. Sci. Downloaded from cdnsciencepub.com by 188.117.216.235 on 07/27/23

probability of entering a new river basin in the physical environment was linked to the distance separating the new river basin from the natal river. Then, relatively to the pairwise distances, a weight was assigned to each river basin using a logit function with most parameters defined as model parameters (see Table A1 and eq. A3 for more details). All the weights were then standardized so that the sum of weights equaled 1 providing the probability for each river basin to be selected. Migrating spawners then entered the specific river basin, survived, and reproduced if they found suitable thermal conditions.

At each time step, the probability of survival for each individual was estimated using its location along the land–sea continuum. The seasonal survival probability accounted for annual mortality coefficients at sea and in the river, with the latter depending on the water temperature. After reproduction, the probability of survival for spawners was defined by the  $Sp_{sp}$  parameter. As allis shad is a semelparous species and the majority of individuals die after reproduction, the probability of survival was set to a low value of 0.1 (Table A1). Most individuals died after reproduction, with their carcasses remaining in the river to decompose. Surviving spawners returned to the sea to reproduce the following years.

#### Sex differentiation and main improvements of the GR3D model

The amounts of N and P brought by shads into river systems can vary depending on sex because males and females differ in their elemental composition and mass-at-age (Durbin et al. 1979; Taverny 1991). To address this, GR3D was updated to estimate male and female abundances separately. Based on previous studies addressing allis shad population dynamics (Menesson-Boisneau 1990; Menesson-Boisneau et al. 2000), three parameters appeared relevant to differentiate males and females in the model: the optimal growth coefficient ( $K_{optGrow}$ ), the asymptotic length ( $L_{\infty}$ ), and the length at maturity ( $L_{mat}$ ) (Table A1). The values for the three parameters were directly estimated for both genders using a non-linear optimization performed with R studio software (R Core Team 2018) so that the set of parameters best fits the observations of age and length. The differentiation between males and females in GR3D required a doubling of the previous value used for the fecundity parameter ( $\alpha$ ) in the BH-SR relationship that had only considered females. When integrating both sex into the model, the number of spawners needed to reach the asymptotic recruitment increased, leading to change the value of fecundity from 135 000 to 270 000 eggs per female to keep the same BH-SR as in Rougier et al. (2014) (Table A1).

Finally, the river temperature ranges ensuring recruitment and egg survival were also modified to take into account new insights on allis shad spawner and larvae thermal tolerances (Jatteau et al. 2017; Paumier et al. 2019) (Table A1).

#### Environmental and biological data to run simulations

Data regarding the distribution of allis shad used to run simulations were obtained from the EuroDiad 4.0 database, which records the presences and absences of European diadromous species in a total of 350 river basins throughout North Africa, Europe, and the Middle East from 1750 to present day (<https://data.inrae.fr/dataset.xhtml?persistentId=doi:10.15454/IVVAIC>). Based on this updated version of EuroDiad, 135 basins were integrated into the GR3D physical environment to cover the core range of the species. The major addition from Rougier et al. (2014) was the inclusion of the UK and Irish river basins. River basins were distributed along a latitudinal gradient from Morocco (Oum Er-Rbia (33.3°N)) to northern Scandinavia (Vefsna (65.8°N)), including the British Isles (Figure A1). All of the 135 river basins were characterized by seasonal near-atmospheric surface temperatures at the outlet. Near atmospheric surface temperatures from 1901 to 2018 were extracted from the CRU database (<https://crudata.uea.ac.uk/cru/data/hrg/#info>), which consists of an atmospheric interpolated

gridded dataset from weather observations with a resolution of  $0.5^{\circ} \times 0.5^{\circ}$ . Data were provided by the FIC (Fundación para la Investigación del Clima; <https://www.ficlina.org/>) as monthly means and stored as NCDF files. The 135 sea basins located in front of each river basin outlet were characterized by seasonal temperatures calculated as the mean between 12 °C (temperature of the Bay of Biscay sea bottom) and the seasonal temperatures in the associated river basin.

#### Description of simulations

Simulations were run over the period 1800–2010 (i.e., 844 time steps). The model was initialized with an initial population set at 500 000 juveniles in each river basin. Simulations started in the summer of 1800 and were run for 100 years with constant temperature conditions (average temperatures of the 1901–1910 decade) to populate the model and limit the influence of initial conditions on simulations. Then, the model was run from 1900 to 2010 with updated seasonal temperature time series described in above section “Environmental and biological data to run simulations”. At each time step, the model provided estimates of shad abundances in each river basin (e.g., total abundance, abundance of male and female spawners), as well as information on population status, dynamics, and spatial distribution (e.g., number of juveniles in each river basin, colonization range and number of river basins colonized). For the purpose of this study, we focused on the early 20th century, so only seasonal estimates of the first 30 years are presented in the results (i.e., 1900–1930). This period was selected because it refers to a “pristine” situation, in which there was no clear evidence for shifts in the state and functioning of natural systems driven by human activities (also called “the Great Acceleration” of the Anthropocene; Steffen et al. 2015). For shads, the “pristine situation” specifically hinted that populations were still abundant and did not suffer from major human impacts or climate change. Since no anthropogenic pressures were accounted for in the GR3D model, simulation outputs corresponded to a maximum “potential” in terms of fish and nutrients. Simulations were run until 2010 so that model estimates could be compared to observations of shad abundances, as described in the next section.

#### Partial validation of estimated fish abundances

Nutrient estimates were a function of fish abundances, so it was relevant to test the robustness of GR3D estimates. To do so, model outputs were compared to observed abundances for a set of 13 well-studied river basins located in France, Portugal, and Spain, for which time series of annual abundances were available (Fig. A1). Observations of shad abundances were given for different time periods depending on data availability and monitoring status of the 13 rivers. For most rivers, observations ranged from the end of the 1990s to the early 2000s, with an exception for the Minho River benefiting from fisheries time series dating back to 1914. For each of the 13 rivers, annual abundances were averaged over the sampling period to be compared with abundances derived from our model from the same time range. Data regarding allis shad spawner abundance in these rivers were either derived from fisheries landings, video counting systems at fishways or based on the number of spawning events recorded at the spawning grounds (“splash-based” method). All the data and methods used to estimate observed abundances were fully described in Appendix A.

To assess the coherence between model estimates and observed values, we classified model estimates into four categories. Rivers for which estimates were lower than observations were in “Category 1”. Rivers for which estimates were higher than observations pertained to categories from 2 to 4 depending on how far estimates were from observations. The category number increased with the magnitude of the difference (i.e., less than two (Category 2), less than ten (Category 3), or more than ten times (Category 4)). As no

anthropogenic pressures were included in the simulations, model estimations were considered as “validated” when the output value for a given basin was greater than the observed value but of the same order of magnitude (Categories 2 and 3).

**Design of the nutrient routine**

The amounts of N and P conveyed by shads were calculated seasonally in each of the 135 rivers through the development of a nutrient calculator implemented in the GR3D model. The routine computes nutrient loads based on the number of living and dead individuals simulated each season. The net nutrient amount  $F_j^n$  provided by shads during their seasonal reproductive migration in a given basin  $j$  was calculated as the difference between the nutrient imported by migrating spawners  $I_j^n$  and nutrient exported by out-migrating juveniles  $E_j^n$  (eq. 1). The dynamics of nutrient imports provided by adults was examined in the context of shad reproductive and dispersal processes. Therefore, considering a total nutrient influx of N and P in the river  $j$ , we distinguished the contribution of fish produced by the river (hereinafter called “autochthonous”) from the contribution of fish coming from other rivers (hereinafter called “allochthonous”; see section below on “Quantifying nutrient interdependencies among river basins”).

$$(1) \quad F_j^{n \in \{N,P\}} = \sum_{k \in \{\text{auto}, \text{allo}\}} I_{k,j}^n - E_j^n$$

with “auto” and “allo” corresponding to autochthonous and allochthonous fish, respectively, as presented in the section below: “Quantifying nutrient interdependencies between river basins”.

**Quantifying nutrient imports**

Following the approaches of Haskell (2018) and Barber et al. (2018), it was assumed that adults were not feeding after entering rivers to only account for marine-derived nutrient inputs. A fish that has successfully migrated to a river after growing and maturing at sea is likely to (i) die before reaching the spawning grounds and reproducing, (ii) die after reproduction (i.e., semelparous fish), or (iii) survive both reproduction and migration back to the sea (i.e., iteroparous fish). Fish that died prior to or after reproduction were considered as providing the same amount of nutrient inputs. Consequently, total nutrient import  $I_{k,j}^n$  corresponded to the sum of the imports from fish dying either before or after reproduction  $Id_{k,j}^n$  and fish surviving  $Is_{k,j}^n$  the reproduction season (eq. 2), regardless of whether they were autochthonous or allochthonous:

$$(2) \quad I_{k,j}^n = Id_{k,j}^n + Is_{k,j}^n$$

The main sources of nutrient inputs in river basins were assumed to be carcass decomposition, gamete emission, and fish excretion. As there was limited field data available for allis shad, carcasses inputs were computed using the average mass of male and female fish that died before spawning (eq. 3). Gamete contribution was hence implicitly considered in the average total mass of the adults, which included both somatic and unspawned gonadic mass.

$$(3) \quad Id_{k,j}^n = \sum_{s \in \{\text{male}, \text{female}\}} Nd_{k,s,j} \times W_s \times (\eta_s^n + RT \times \tau^n)$$

where  $Nd_{k,s,j}$  is either the number of male or female spawners (both autochthonous and allochthonous) that died before or after reproduction in a given river basin  $j$ ,  $W_s$  is the average total mass of a male or female spawner,  $\eta_s^n$  is their nutrient content (%N and %P), RT is an estimate of the residence time defined as the average number of days that a fish spent in fresh water, and  $\tau^n$  is the excretion rate of an adult for the nutrient considered.

**Table 1.** Inputs used in the nutrient routine for allis shad.

Measurements	Nominal values			
	$\alpha$	$b$	%N (wet) <sup>b</sup>	%P (wet) <sup>b</sup>
<b>Female</b>				
$W^a$	$2.6654 \times 10^{-3}$	3.343	2.958	0.673
Pre-spawn ovary <sup>c</sup>	$528.702 \times 10^{-5}$	2.673	3.242	0.320
Post-spawn ovary <sup>c</sup>	$132.890 \times 10^{-5}$	2.854	—	—
<b>Male</b>				
$W^a$	$4.0958 \times 10^{-3}$	3.225	2.941	0.666
Pre-spawn teste <sup>c</sup>	$13.9926 \times 10^{-5}$	3.384	3.250	0.724
Post-spawn teste <sup>b</sup>	$1.2560 \times 10^{-5}$	3.833	—	—
<b>Juvenile</b>				
$W_o^a$	$6.9864 \times 10^{-3}$	3.031	2.803	0.887

**Note:** The two parameters  $\alpha$  and  $b$  were derived from weight-length relationships. Data sources from which model inputs were derived are indicated in the footnotes.

<sup>a</sup>Taverny (1991).

<sup>b</sup>Haskell (2018).

<sup>c</sup>Computed from data provided by MIGADO (<http://www.migado.fr/>).

$W$  was estimated for both sexes as a function of adult mean length  $L$  following the relationship  $W = \alpha L^b$ , with  $\alpha$  and  $b$  derived from Taverny (1991) (Table 1). The original relationship was given in  $g \cdot mm^{-1}$ , so it was converted to  $g \cdot cm^{-1}$  (eq. 4a and eq. 4b).

$$(4a) \quad W_m = 4.0958 \times 10^{-3} \times L_m^{3.2252}$$

$$(4b) \quad W_f = 2.6654 \times 10^{-3} \times L_f^{3.3429}$$

Nutrient percent contents  $\eta^n$  were taken from studies on American shad as no data was available for allis shad, with  $\eta_m^N = 0.02941$  and  $\eta_m^P = 0.00666$  for males and  $\eta_f^N = 0.02958$  and  $\eta_f^P = 0.0067$  for females (Haskell 2018). Likewise, the excretion rate  $\tau$  of  $2.17 \times 10^{-6} \mu g \text{ N}$  and  $24.7171 \times 10^{-5} \mu g \text{ P} \cdot g \text{ wet fish mass}^{-1} \cdot h^{-1}$  were based on results for alewife (Post and Walters 2009) (Table 1). Those values were converted in g and then multiplied by 24 h to calculate a daily input. The residence time RT was assumed to be the same regardless of when fish dies and was fixed to 30 days according to shad ecology (Olney et al. 2006; Aunins and Olney 2009).

For iteroparous individuals that survive reproduction, nutrient imports are only a function of gamete inputs and excretion (eq. 5).

$$(5) \quad Is_{k,j}^n = \sum_{s \in \{\text{male}, \text{female}\}} Ns_{k,s,j} \times W_{g,s} \times (\eta_{g,s}^n + RT \times \tau^n)$$

where  $Ns_{k,s,j}$  is either the number of male and female spawners (both autochthonous and allochthonous) surviving reproduction in basin  $j$ ,  $W_{g,s}$  is the wet mass of testes or ovaries and  $\eta_{g,s}^n$  is the nutrient content (%N and %P) of male or female gonads. The total wet mass of gamete inputs  $W_g$  was estimated as the difference between spawned and unspawned gonad masses, which were both modeled as a function of length (Table 1; eqs. 6a and 6b). As previously defined for carcass weight  $W$ , separate weight-length relationships were defined for each sex. For the unspawned gonad mass, both relationships were derived from fish captured during the 2008–2018 period at Golfech and Tuilières dams on the Garonne and Dordogne rivers, respectively. The relationships for spawned gonad mass were derived from the same geographical location after artificial reproduction at the Bruch experimental station. Data were obtained from the nonprofit association MIGADO (<http://www.migado.fr/>).

Can. J. Fish. Aquat. Sci. Downloaded from cdnsciencepub.com by 188.117.216.235 on 07/27/23

$$(6a) \quad W_{g,m} = 13.9926 \times 10^{-5} \times L_m^{3.3838} - 1.2560 \times 10^{-5} \times L_m^{3.8331}$$

$$(6b) \quad W_{g,f} = 528.702 \times 10^{-5} \times L_f^{2.6729} - 132.890 \times 10^{-5} \times L_f^{2.8545}$$

The percent wet mass content of N and P for eggs and sperm were approximated using values for ovaries and testes taken from American shad, with  $\eta_{g,m}^N = 0.0325$  and  $\eta_{g,m}^P = 0.00724$  for males and  $\eta_{g,f}^N = 0.03242$  and  $\eta_{g,f}^P = 0.0032$  for females (Haskell 2018) (Table 1).

### Quantifying nutrient exports

The total export of nutrients conveyed by out-migrating juveniles from the river to the sea was calculated as follows (eq. 7):

$$(7) \quad E_j^n = N_{o_j} \times W_o \times \eta_o^n$$

The offspring abundance  $N_{o_j}$  in basin  $j$  derived from GR3D was multiplied by the wet mass of juvenile  $W_o$  and its nutrient content  $\eta_o^n$  (%N and %P). As was done for adults spawners, the wet mass of juveniles was described as a function of juvenile length  $L$  and was based on the relationship derived from Taverny (1991) (Table 1):

$$(8) \quad W_o = 6.9864 \times 10^{-3} \times L^{3.0306}$$

The percent nutrient content of emigrating juveniles was provided by Haskell (2018) as  $\eta_o^N = 0.028$  and  $\eta_o^P = 0.00887$ .

### Quantifying nutrient interdependencies among river basins

Nutrient inputs supported by the population dynamics of spawners across the 135 river basins were computed based on the natal origin of individuals (i.e., donor basins, where fish were born) and the destination where fish are showing up to spawn (i.e., recipient basins, where spawner migrate to reproduce). When the natal basin was also the destination basin, fish were considered “autochthonous”. On the other hand, when the natal and destination basins were different, fish were labelled as “allochthonous”. Autochthonous fish were homers (i.e., fish coming back to their natal river basin to reproduce), while allochthonous fish were strayers wandering from other river basins. So, for each destination basin  $j$ , the import of N and P was computed as the inputs provided by autochthonous fish that either die or survive after reproduction ( $Id_{j,auto}^n$ ,  $Is_{j,auto}^n$ ) and those related to allochthonous fish ( $Id_{j,allo}^n$ ,  $Is_{j,allo}^n$ ).

The relative nutrient contribution between autochthonous and allochthonous fish was related to the species dispersal dynamics. For this modeling attempt, we considered the same homing fidelity for all the rivers, so that 75% of fish returned to the natal river to spawn ( $p_{hom}$  set to the high value of 0.75; see Table A1 and Rougier et al. (2014) for more details). For strayers, the probability of migrating to a destination basin increased as the distance between natal and destination basins decreased. Therefore, it was more likely for a fish to spawn in neighboring basins than basins located far away from the natal river, as explained in above in the section “Population dynamics within the model”.

For each destination basin, the annual input of N and P was averaged over the period 1900–1930 to provide an average estimate of the “maximal potential” for fish to deliver nutrients over this period (eq. 9):

$$(9) \quad \bar{I}_j^n = \frac{1}{31} \times \sum_{t=1900}^{1930} Id_{j,auto}^n(t) + Is_{j,auto}^n(t) + Id_{j,allo}^n(t) + Is_{j,allo}^n(t)$$

The nutrient inputs supported by allochthonous fish (i.e., strayers) over the 135 river basins were represented with a Chord Diagram using the R package “Circlize” (Gu 2014; <https://CRAN.R-project.org/package=circlize>) widely used in population dynamics and genetics

to quantify human migrations or gene flows. River basins were displayed all around a circle and connected with links corresponding to nutrient subsidies related to allochthonous fish. An in-depth analysis of the nutrient dynamics at the river-basin scale was performed using the Garonne River as a case study because the Garonne River was the reference population for shad in Europe and, as such, was carefully studied by the scientific community. Nutrient subsidies moving in and out of the Garonne River basin were represented with a Sankey diagram using the R package “networkD3” (Allaire et al. 2017; <https://CRAN.R-project.org/package=networkD3>). Similar to the range-scale analysis, this method allows displaying the amount of nutrients supplied by fish migrating from one river to another with arrows indicating the magnitude of these inputs.

## Results

### Partial validation of abundance estimates

For the 13 river basins used to assess the global accuracy of model outputs, estimates of abundance provided by the GR3D model were higher than the observed values in almost all river basins (85%) except for the Vire and Orne rivers in France (Table 2). Nonetheless, the differences in order of magnitude between observations and simulations were highly variable across river basins, reflecting, to some extent, the variety of observational data used for comparison through the study area. Almost half of the 13 river basins (48%) were classified in Category 4, for which model outputs were much higher (i.e., above ten times higher) than the observations and the majority of the remaining river basins (38%) were placed into intermediate categories 2 and 3, for which model outputs and observations were of the same order of magnitude.

### Nutrient dynamics in the Garonne River basin case study

Over the 1900–1930 period, allis shad conveyed an average load of  $0.324 \pm 0.048 \text{ kg N}\cdot\text{km}^{-2}\cdot\text{year}^{-1}$  and  $0.055 \pm 0.008 \text{ kg P}\cdot\text{km}^{-2}\cdot\text{year}^{-1}$  in the Garonne River basin. Shad were net importers of N and P, as the total amount of nutrient subsidies brought by spawners was higher than nutrients exported by out-migrating juveniles ( $0.003 \pm 7.862 \times 10^{-4} \text{ kg N}\cdot\text{km}^{-2}\cdot\text{year}^{-1}$  and  $9.621 \times 10^{-4} \pm 2.488 \times 10^{-4} \text{ kg P}\cdot\text{km}^{-2}\cdot\text{year}^{-1}$ ). Regarding the source–sink dynamics, most shad-derived nutrients were imported by autochthonous fish (97.1% of the total nutrient imports) and, to a lesser extent, by fish originating from neighboring river basins such as the Dordogne (1.91%), Charente (0.47%), and Loire (0.21%) rivers (Fig. 2). The other donor river basins contributed less than 0.1% each to the amount of nutrients imported in the Garonne over 1900–1930. The Garonne River basin produced more strayers than it received. Most of the strayers from the Garonne River basin migrated to the Charente, Seudre, Dordogne, Lay, Sèvre Niortaise, Auzaunce and Leyre river basins, all in France.

### Nutrient flows at the Atlantic area scale

A noticeable variability in annual net budget (import minus export) was calculated across river basins for both nutrients, ranging from  $8 \times 10^{-6}$  to  $1.2 \times 10^4 \text{ kg N}\cdot\text{km}^{-2}\cdot\text{year}^{-1}$  and  $1.4 \times 10^{-6}$  to  $2.1 \times 10^3 \text{ kg P}\cdot\text{km}^{-2}\cdot\text{year}^{-1}$ . Most river basins received both allochthonous and autochthonous individuals. The contribution of autochthonous individuals to the total import was also highly variable, ranging from 2.09% in the Taff River (UK) to 99.23% in the Loire River (France) (Fig. 3). The Chord Diagram distinguished among river basins that produced more strayers than they received (source-like) and river basins that received more strayers than they produced (sink-like) (Fig. 4). River basins located at the southern edge of the distribution, such as the Guadalquivir, Guadiana, Tagus, and Douro rivers in the Iberian Peninsula, as well as the Loire and Garonne rivers in France, were identified as the main producers of strayers. On the contrary, the Piedras, Tinto, Odiel, and Sado rivers in Spain and Portugal appeared as the main destinations for strayers along the Atlantic Area.

**Table 2.** Comparison between GR3D estimated abundances and observed data for 13 river basins along the European Atlantic coast.

River basin name (country)	Year	Observations		GR3D outputs	
		Abundance (annual mean with minimum and maximum values in number of fish)	Data type	Abundance (annual mean with minimum and maximum values in number of fish)	Quality code
Lima (Portugal)	1990s	3000 (1000–5000)	Fisheries <sup>a</sup>	57 851 (50 036–66 328)	4
Minho (Spain)	1914–1944	78 400 (15 000–105 000)	Fisheries <sup>a,b</sup>	123 761 (100 979–163 581)	2
Nivelle (France)	1998–2008	300 (29–688)	Entrapment–video counting at fishways <sup>c</sup>	6975 (6105–8048)	4
Adour (France)	1985–1999	11 176 (NA)	Professional fisheries <sup>a,d</sup>	86 961 (66 131–112 105)	3
Garonne (France)	1996–2006	94 392 (46 409–161 306)	Video counting at Golfch and splash-based estimations <sup>c</sup>	446 096 (369 249–497 017)	3
Charente (France)	2010–2016 <sup>b</sup>	26 046 (16 893–38 502)	Splash-based estimations <sup>f</sup>	106 831 (90 080–134 357)	3
Loire (France)	1998–2008	10 320 (1200–31 418)	Video counting at fishways <sup>c</sup>	669 405 (555 001–781 317)	4
Vilaine (France)	1996–2006	918 (54–2618)	Video counting at Arzal <sup>c,g</sup>	103 951 (92 436–118 848)	4
Scorff (France)	1996–2006	39 (2–188)	Entrapment–video counting at Moulin des Princes <sup>g</sup>	28 501 (24 810–33 057)	4
Aulne (France)	2000–2010	3353 (399–6714)	Video counting at Chateaulin <sup>c,g</sup>	8967 (7229–10 005)	3
Elorn (France)	2007–2010	380 (202–508)	Video counting at Kerhamon <sup>c,g</sup>	4464 (4273–4735)	4
Vire (France)	2002–2010	4258 (1751–8000)	Video counting at Claiès de Vire <sup>c,g</sup>	198 (109–276)	1
Orne (France)	2002–2010	201 (50–406)	Video counting at Feuguerolles <sup>c,g</sup>	51 (28–74)	1

**Note:** Seasonal model outputs and observations were averaged over the same time period, with minimum and maximum values provided. River basins were ordered by latitude from Portugal to France. A quality code ranging from Category 1 to Category 4 was used to highlight the agreement between model estimates and observed values. Category 1 indicated model outputs were lower than observed values and thus judged as inaccurate. Categories 2, 3, and 4 indicated model outputs were higher than observed values with increasing differences. The highest agreement was seen for intermediate categories 2 and 3. Data sources are indicated in the footnotes.

<sup>a</sup>ICES (2015).

<sup>b</sup>Mota (2014).

<sup>c</sup>P. Jatteau (personal observations, 2015).

<sup>d</sup>Baglinière and Élie (2000).

<sup>e</sup>Logrami (<http://www.logrami.fr/>).

<sup>f</sup>EPTB Charente (<https://www.fleuve-charente.net/>).

<sup>g</sup>Plagepomi (<https://www.observatoire-poissons-migrateurs-bretagne.fr/>).

<sup>h</sup>GR3D estimates were provided for the 1996–2006 period, as there is no temperature available after 2010 in the CRU database.

## Discussion

### Strengths and limits of the methodology

By combining a nutrient routine with a mechanistic species distribution model, the capacity of shad to move N and P subsidies between marine and freshwater ecosystems across their distribution range was quantitatively assessed. This work constituted one of the first evaluations of the regulating services associated with a diadromous fish species across its distribution range. Compared to river basin-specific assessments, this study brought substantial insights into the interdependencies among river basins regarding nutrient supplies related to anadromous species.

As our model was calibrated on historical presences and absences, abundance estimates provided by the model required validation using observed data (Table 2). These results suggested a somewhat limited agreement between model outputs and existing data, with estimated abundances much higher than observations in half of the 13 river basins used for validation (i.e., Category 4). For rivers with monitoring data included both shad species, model overestimation would likely be higher by considering a relatively low number of allis shad. However, the model coherence would remain the same, according to the validation index used. One explanation for these large differences is that reliable monitoring of shad populations started at the end of the 20th century (after 1950), when significant declines in most spawning stocks had already occurred. The GR3D simulations did not integrate anthropogenic pressures, meaning that abundance estimates represented a “maximum potential”. In addition, observations were mostly based on a single data source that cannot be representative of the overall fish stock. For abundance estimates derived from counting at fishways, the data reliability is depending on the location of the device. If fish mostly spawn downstream of the dam, fish may not cross the barriers and

therefore would not be counted by the device. These points, in addition to any inherent biases in the monitoring data, indicated that the comparison between observed and estimated abundances was only valid if the sign and magnitude of the differences were considered and not the absolute values. Using this criterion, the partial model validation indicated overall confidence in the abundance estimates in the central and southern parts of the species range. However, simulations using previous and current GR3D versions indicated that the model estimates are less reliable throughout the northern range of allis shad, underestimating fish abundances in northern France (the Vire and Orne rivers in Table 2) up to Germany (Rougier et al. 2014).

### The nutrient balance in the Garonne River basin: a local analysis

Our model calculated that allis shad historically imported an average of  $0.324 \pm 0.048$  kg N·km<sup>-2</sup>·year<sup>-1</sup> and  $0.055 \pm 0.008$  kg P·km<sup>-2</sup>·year<sup>-1</sup> in the Garonne River basin. These values are far below the total amounts of N and P loaded from external sources. For instance, the total nutrient export from the Garonne River basin into the coastal zone was estimated to be 5792 t·month<sup>-1</sup> for N and 224 t·month<sup>-1</sup> for P over the period 1991–1995 (Romero et al. 2013). These numbers for allis shad were also lower than the N and P loadings reported for other diadromous species. By comparison, Haskell (2018) found that the closely related American shad (*Alosa sapidissima*) imported over 15 000 kg N and 3000 kg P annually in the John Day Reservoir (JDR) in the lower Columbia River over the 1997–2015 time period. Considering that the JDR has a surface area of 222.6 km<sup>2</sup>, the total amount of N and P associated with American shad spawning runs would be 67.38 kg N·km<sup>-2</sup>·year<sup>-1</sup> and 13.48 kg P·km<sup>-2</sup>·year<sup>-1</sup>. However, these estimates were for a specific reservoir within the Columbia River watershed, while the nutrients subsidized by allis shad were for the entire Garonne

**Fig. 2.** Sankey diagram of the nitrogen flows associated with the Garonne River basin. All the river basins listed on the left were “natal basins”, and all the river basins on the right were “destination basins”. The light grey band represented fish originating from the Garonne River basin and returning to the Garonne River basin (autochthonous fish). The four lines at the bottom indicated the origins of the allochthonous fish entering the Garonne River basin. Lines above the light grey band indicated the destinations of Garonne strayers in the Atlantic area. Lines were proportional to the net nitrogen import. River basins on the right were ordered by latitude, with the exception of the Garonne River basin.

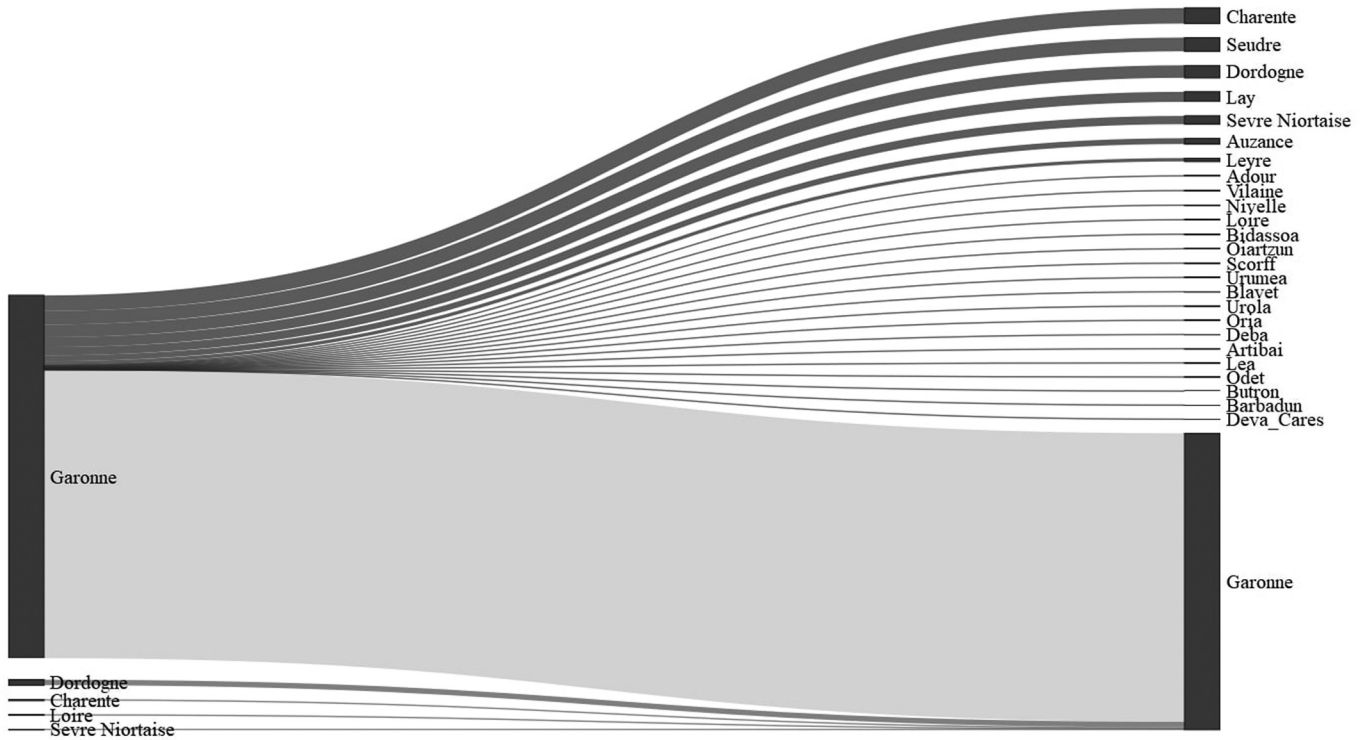
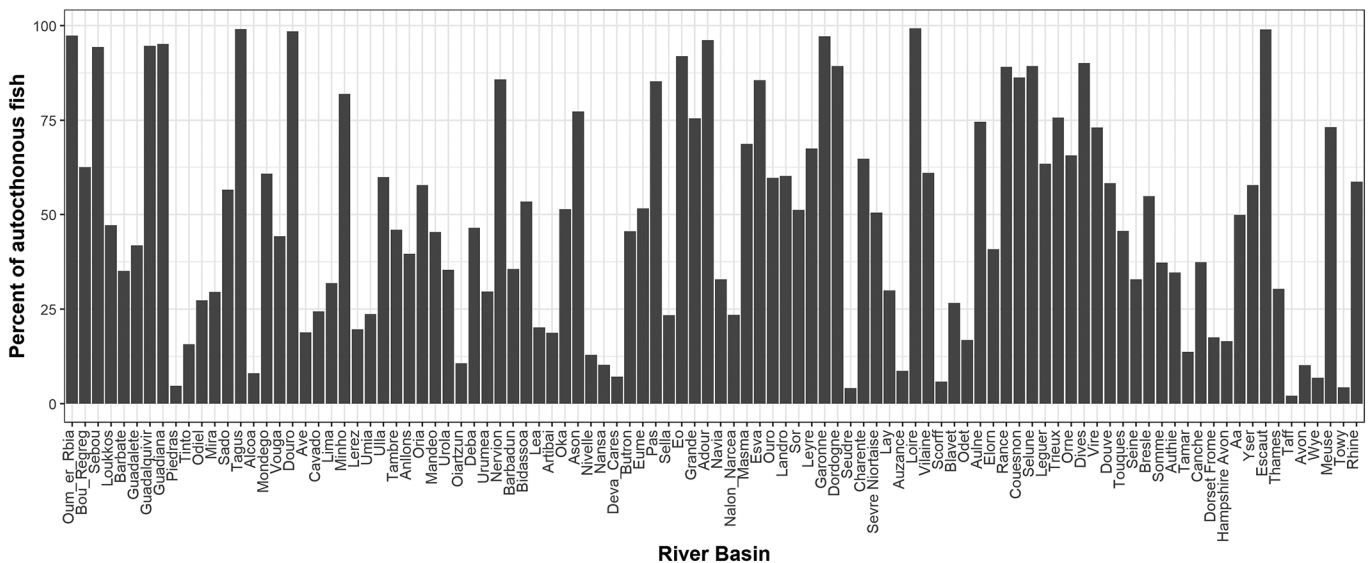


**Fig. 3.** Contribution of the autochthonous fish (in %) to the total import of nitrogen over the period 1900–1930 in the river basins colonized by shads in the GR3D physical environment. The remaining percent was for inputs derived from strayers coming from other rivers. River basins were ordered along a latitudinal gradient from Morocco to Germany.



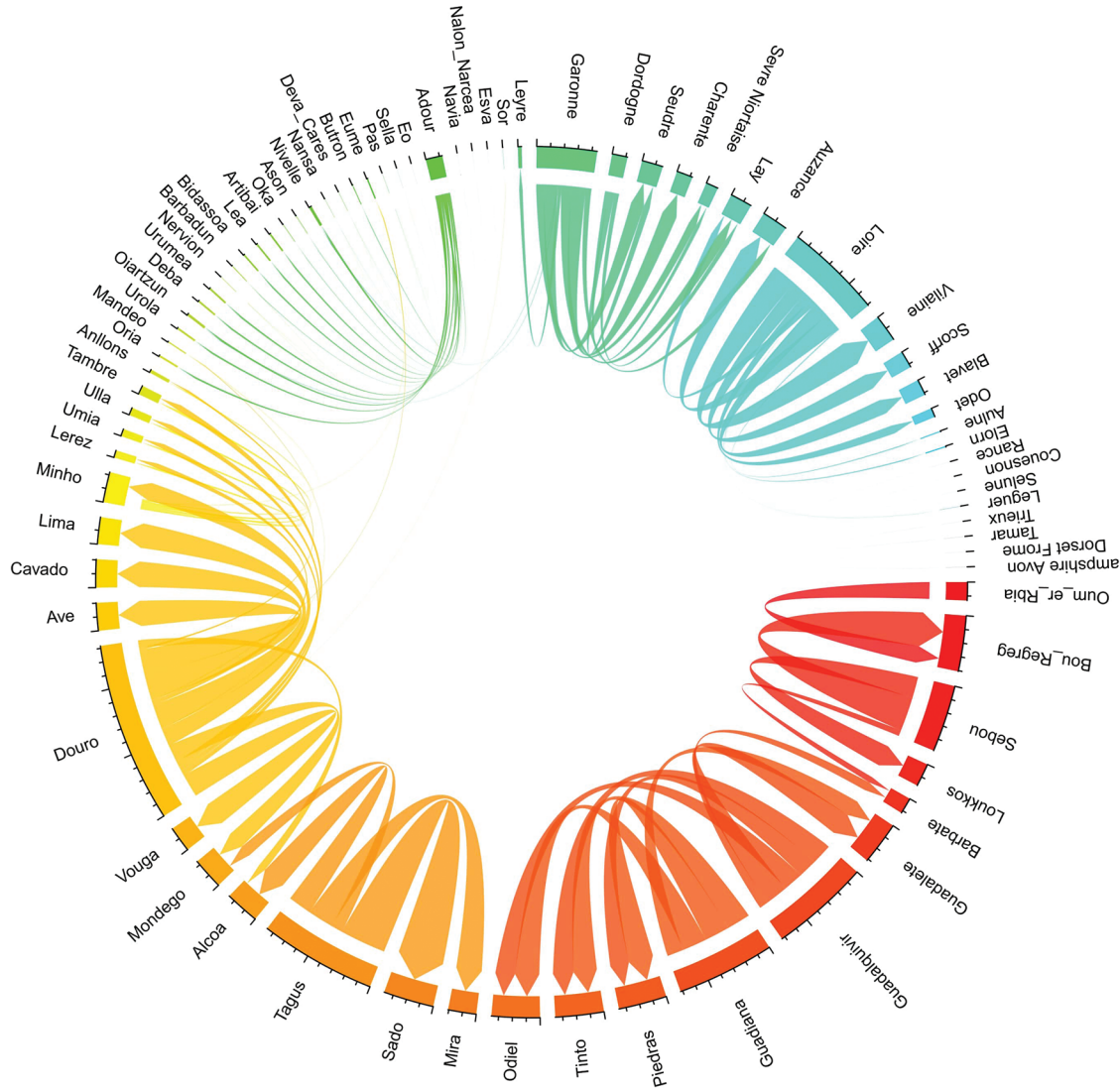
watershed. To be consistent, nutrient estimates must be displayed at a similar scale. Considering water surface only covers 1% of the whole Garonne River watershed (BD TOPAGE: <https://bdtopage.eaufrance.fr/>), the amount of N and P load by allis shad population would be over 31.130 kg N·km<sup>-2</sup>·year<sup>-1</sup> and 5.290 kg P·km<sup>-2</sup>·year<sup>-1</sup>.

These values were still below those founded for the American shad in the JDR but were supported by a smaller population size (467 000 for almost 1 billion entering the JDR; Haskell 2018).

The ecological meaning of these nutrient subsidies is a function of the baseline nutrient levels of riverine waters. For oligotrophic

Can. J. Fish. Aquat. Sci. Downloaded from cdsciencepub.com by 188.117.216.235 on 07/27/23

**Fig. 4.** Interdependencies among river basins in nitrogen supplies provided by allochthonous allis shad straying from one to another river (kg N) over the period 1900–1930. Each intermediate tick mark increases by 800 kg N, starting from 0. River basins were ordered clockwise along a latitudinal gradient, ranging from the Oum Er-Rbia river basin at the southern edge of the distribution in Morocco (red) to the Avon River basin at the northern edge of the distribution in the UK (blue). To ease interpretation, only the nitrogen supplies provided by allochthonous fish contributing more than 10% of the total nutrient subsidies imported in each river basin were represented in the figure. The magnitude and flow of each relationship were indicated by arrow size and direction, respectively. A latitudinal colour gradient was used to distinguish among arrows from different basins. The contribution of autochthonous fish was not represented in the Chord Diagram.



ivers where N and P tend to be limiting resources, even low levels of enrichment by migratory organisms such as shad would be significant enough to increase the ecosystem productivity (Durbin et al. 1979). Although, for the Garonne River, the significance of these nutrient subsidies should be examined by considering the timing to which resources are delivered and where. Anadromous species spawn seasonally in specific and restricted areas, so they provide a condensed pulse of nutrients over a short period of time (Weber and Brown 2018). In rivers, the availability of N and P to an aquatic organism varies according to its trophic status, the season, riverine inputs, and biogeochemical and bacterial activity.

Along the European Atlantic coast, allis shad spawn in the spring when primary productivity in rivers is starting to increase, and riverine inputs of N and P from upstream reaches start to become relatively low due to decreasing river discharge. Under

such environmental conditions, carcasses were unlikely to be washed out or moved downstream over substantial distances from the spawning grounds (Garman 1992). Hence, carcass decomposition may provide a relatively steady source of nutrients for several weeks, and N and P subsidies delivered in spring and summer may have a larger impact on ecosystem functioning than suggested by the total annual amounts alone.

This study provided the first quantification of nutrient fluxes transported by allis shad from marine to freshwater ecosystems at the distribution range scale, but it did not investigate the trophic pathways of marine-derived nutrients incorporation into riverine food webs. Previous studies have explored the contribution of fish-derived nutrients into riverine and lacustrine food webs using stable isotope analyses (Kohler et al. 2012; Guyette et al. 2014; Samways et al. 2018). Marine-derived nutrients enter food webs either through direct consumption of marine-derived

Can. J. Fish. Aquat. Sci. Downloaded from cdnsciencepub.com by 188.117.216.235 on 07/27/23

organic matter (e.g., carcasses or eggs) by predators and scavengers or through indirect uptake of dissolved nutrients by bacteria and other autotrophic organisms (Samways et al. 2018). For several anadromous species, both pathways were suggested as a primary source of nutrients, depending on the location of populations. In a small Alaskan system, Gende et al. (2004) demonstrated that almost 50% of the salmonids derived-nutrients in the stream was directly incorporated into the riverine food web through predation by bears. Like salmonids, alewives may also subsidize higher trophic levels directly as a food resource for a wide variety of aquatic predators (Flecker et al. 2010) or may be incorporated via the bottom-up trophic pathways. For instance, Walters et al. (2009) showed that the indirect uptake by periphyton of dissolved nutrients released from excretion and carcass decomposition was then delivered to higher trophic levels such as macroinvertebrates.

So far, the contribution of allis shad to riverine food webs remains unexplored. Given the species' semelparous existence, with most fish dying after reproduction, allis shad-derived nutrients would be first incorporated through direct consumption of carcasses by macroinvertebrates (Fenoglio et al. 2010). In the Rappahannock River system (Virginia), MacAvoy et al. (2000) did not find evidence of shad-derived marine nutrients at lower trophic levels, suggesting that shad would have a greater influence acting as prey for carnivorous fish and birds (Garman and Macko 1998; MacAvoy et al. 2000; Haskell 2018).

#### Diadromous species as valuable cross-border resources

By examining the nutrient dynamics related to shad throughout its entire distribution range, this study mapped the main locations of nutrient provision and destination across the European coast of the Atlantic Ocean. Most river basins in GR3D received substantial N and P subsidies imported by strayers from the marine system, suggesting that each river basin supports the provision of ecosystem services in other locations but some more than others. Since the straying rate was the same for all the river basins considered, these differences were mainly driven by the size of the catchment. Large catchments produced more spawners and thus more individuals that would stray to nearby rivers. Similarly, depending on the location of the rivers along the Atlantic arc, the size, and the number of neighboring basins, contributions of autochthonous or allochthonous species are expected to change accordingly.

These findings are partly corroborated by the study conducted by Randon et al. (2018). Using otolith microchemistry and a Bayesian approach, these authors identified major "source" and "sink" subpopulations across 18 rivers sampled in France and Portugal. Results suggested that multiple exchanges occurred among rivers, contrasting with the high level of homing presumed for this species (Jolly et al. 2012; Martin et al. 2015). In their study, the Dordogne and Minho rivers appeared to be sources, defined as a river "which produced more individuals than received", while the Loire, Garonne, and Mondego rivers received a high percent of strayers compared to homers. The Garonne River basin appeared as a main sink with 99.9% of fish being strayers from neighboring rivers. Conversely, the present modeling results revealed that 98% of N and P inputs in the Garonne River basin were historically provided by homers. Nonetheless, in the current study, most of the allochthonous spawners coming to the Garonne river basin were, in fact, born in the Dordogne River basin, as was seen in the study of Randon et al. (2018). In addition, some of the largest river basins such as the Douro and Tagus in Portugal, known as important allis shad populations, were not considered by Randon et al. (2018), forcing the reallocation by the Bayesian model of adults into other chemically similar rivers and limiting the interpretation of exchanges based on microchemistry analyses.

These two studies put together confirmed that conservation efforts in the Gironde-Garonne-Dordogne system would benefit from the recognition of linkages between these two river basins

even if the intensity of this relationship is still to be determined. More broadly, the amount of nutrient flow sustained by the meta-population dynamics of spawners in the present study argues for cross-border cooperative management efforts instead of catchment-specific measures ([www.diades.eu](http://www.diades.eu)).

#### Implications for management in a globally changing environment

The management of migratory species is a complex issue as it raises questions on the scale necessary for such operations (Runge et al. 2014). As seen in the present results, the significant exchanges of individuals among river basins, delivering and receiving nutrient subsidies from fish produced at various locations, confirmed the need to shift from local (river basin-specific) to cross-jurisdictional and cross-border cooperative strategies for managing allis shad populations (Semmens et al. 2011; [www.diades.eu](http://www.diades.eu)). This change of perspective is especially urgent when considering the shifts in distribution observed and predicted for many animal and plant species under climate change, including diadromous species impacted by changes in temperature and precipitation patterns (Parmesan and Yohe 2003; Lassalle and Rochard 2009). The situation is obviously changing, causing new socioeconomic and ecological interactions among territories that might increase the spatial mismatches between areas where services are produced and consumed (Semmens et al. 2011).

This study provided estimates of the maximum capacity of shad to convey nutrients across the landscape. However, despite abundant shad stocks calculated by the model in the early 20th century with no anthropogenic pressures at play, the level of nutrients delivered by "pristine" populations seemed low compared to those estimated for other related species and from other sources (e.g., atmospheric deposition, fertilizers, and wastewater). However, one should consider the timing of such inputs (i.e., spring-summer) and the concentration of fish at specific places (i.e., spawning grounds) before concluding that allis shad provide a negligible nutrient subsidy. Considering the massive decline of spawning populations that occurred over the last century and the projected reduction in fish body size (Daufresne et al. 2009), nutrient inputs could be even more reduced by the end of the century (Twining et al. 2017).

#### Contributors' statement

All authors contributed to the study conceptualization and writing. A first draft was written by CP, and then all authors commented on previous versions of the manuscript. All authors read and approved the final manuscript. CP and PL contributed to the software development.

#### Funding statement

This research was co-funded by Agence de l'Eau Adour Garonne and Nouvelle Aquitaine Region within the SHAD'EAU/FAUNA projects (coordination: Françoise Daverat (INRAE)) and the Atlantic Area Interreg Project DiadES (coordination: Géraldine Lassalle (INRAE) and Patrick Lambert (INRAE)).

#### Competing interests statement

The authors declare there are no competing interests.

#### Data availability statement

The updated GR3D code can be openly accessed at <http://doi.org/10.5281/zenodo.4442030> or directly following the URL <https://github.com/inrae/GR3D/tree/v3.2.1>.

#### Acknowledgements

This study was co-funded by Agence de l'Eau Adour Garonne and Nouvelle Aquitaine Region within the SHAD'EAU/FAUNA

projects (coordination: Françoise Daverat (INRAE)) and the Atlantic Area Interreg Project DiadES (coordination: Géraldine Lassalle (INRAE) and Patrick Lambert (INRAE)). Many thanks go to the Fundación para la Investigación del Clima (FIC; <https://www.ficlima.org/>) for providing the CRU database temperature extraction. We are grateful to the French nonprofit association MIGADO (<http://www.migado.fr/>) for giving us access to shad biological characteristics at the Bruch experimental station. We also thank Sébastien Boutry (INRAE) for his sound advices in data visualization technics and the two anonymous reviewers for their constructive remarks on the manuscript.

## References

- Allaire, J.J., Gandrud, C., Russell, K., and Yetman, C.J. 2017. NetworkD3: D3 JavaScript Network Graphs from R. R package version 0.4. Available from <https://CRAN.R-project.org/package=networkD3>.
- Auer, S.K., Anderson, G.J., McKelvey, S., Bassar, R.D., McLennan, D., Armstrong, J.D., et al. 2018. Nutrients from salmon parents alter selection pressures on their offspring. *Ecol. Lett.* **21**(2): 287–295. doi:10.1111/ele.12894.
- Aunins, A., and Olney, J.E. 2009. Migration and spawning of American shad in the James River, Virginia. *Trans. Am. Fish. Soc.* **138**: 1392–1404. doi:10.1577/T08-1601.
- Baglinière, J.-L., and Élie, P. 2000. Les aloses, *Alosa alosa* et *Alosa fallax* spp.: écobiologie et variabilité des populations. Institut national de la recherche agronomique, Paris.
- Bal, G., Rivot, E., Prévost, E., Piou, C., and Baglinière, J.L. 2011. Effect of water temperature and density of juvenile salmonids on growth of young-of-the-year Atlantic salmon *Salmo salar*. *J. Fish Biol.* **78**(4): 1002–1022. doi:10.1111/j.1095-8649.2011.02902.x.
- Barber, B.L., Gibson, A.J., O'Malley, A.J., and Zydlewski, J. 2018. Does what goes up also come down? Using a recruitment model to balance alewife nutrient import and export. *Mar. Coast. Fish.* **10**(2): 236–254. doi:10.1002/mcf2.10021.
- Beverton, R.J.H., and Holt, S.J. 1957. On the dynamics of exploited fish populations. H.M. Stationery Off, London.
- Bilby, R.E., Franssen, B.R., and Bisson, P.A. 1996. Incorporation of nitrogen and carbon from spawning coho salmon into the trophic system of small streams: evidence from stable isotopes. *Can. J. Fish. Aquat. Sci.* **53**(1): 164–173. doi:10.1139/f95-159.
- Bolster, W.J. 2008. Putting the ocean in Atlantic history: maritime communities and marine ecology in the Northwest Atlantic, 1500–1800. *Am. Hist. Rev.* **113**(1): 19–47. doi:10.1086/ahr.113.1.19.
- Castelnaud, G., Rochard, E., and Le Gat, Y. 2001. Analyse de la tendance de l'abondance de l'aloise *Alosa alosa* en gironde à partir de l'estimation d'indicateurs halieutiques sur la période 1977-1998. *Bull. Fr. Pêche Piscic.* **362-363**: 989–1015. doi:10.1051/kmae:2001032.
- Daufresne, M., Lengfellner, K., and Sommer, U. 2009. Global warming benefits the small in aquatic ecosystems. *Proc. Natl. Acad. Sci. USA.* **106**(31): 12788–12793. doi:10.1073/pnas.0902080106.
- Drouineau, H., Carter, C., Rambonilaza, M., Beaufaron, G., Bouleau, G., Gassiati, A., et al. 2018. River continuity restoration and diadromous fishes: much more than an ecological issue. *Environ. Manage.* **61**(4): 671–686. doi:10.1007/s00267-017-0992-3. PMID:29330607.
- Dumoulin, N. 2007. SimAquaLife: un cadriciel pour la modélisation de la dynamique spatiale d'organismes aquatiques. *Tech. Sci. Inform.* **26**(6): 701–721. doi:10.3166/tsi.26.701-721.
- Durbin, A.G., Nixon, S.W., and Oviatt, C.A. 1979. Effects of the spawning migration of the Alewife, *Alosa pseudoharengus*, on freshwater ecosystems. *Ecology*, **60**(1): 8–17. doi:10.2307/1936461.
- Fenoglio, S., Bo, T., Cammarata, M., Malacarne, G., and Del Frate, G. 2010. Contribution of macro- and micro-consumers to the decomposition of fish carcasses in low-order streams: an experimental study. *Hydrobiologia*, **637**: 219–228. doi:10.1007/s10750-009-9998-z.
- Flecker, A., McIntyre, P.B., Moore, J.W., Anderson, J., Taylor, B., and Hall, R. 2010. Migratory fishes as material and process subsidies in riverine ecosystems. *Am. Fish. Soc. Symp.* **73**: 559–592.
- Garibaldi, A., and Turner, N. 2004. Cultural keystone species: implications for ecological conservation and restoration. *Ecol. Soc.* **9**(3): 1. doi:10.5757/ES-00669-090301.
- Garman, G.C. 1992. Fate and potential significance of postspawning anadromous fish carcasses in an Atlantic coastal river. *Trans. Am. Fish. Soc.* **121**(3): 390–394. doi:10.1577/1548-8659(1992)121<0390:FAPSOP>2.3.CO;2.
- Garman, G.C., and Macko, S.A. 1998. Contribution of marine-derived organic matter to an Atlantic coast, freshwater, tidal stream by anadromous clupeid fishes. *J. N. Am. Benthol. Soc.* **17**(3): 277–285. doi:10.2307/1468331.
- Gende, S.M., Quinn, T.P., Willson, M.F., Heintz, R., and Scott, T.M. 2004. Magnitude and fate of salmon-derived nutrients and energy in a coastal stream ecosystem. *J. Freshw. Ecol.* **19**(1): 149–160. doi:10.1080/02705060.2004.9664522.
- Gilligan-Lunda, E.K., Stich, D.S., Mills, K.E., Bailey, M.M., and Zydlewski, J.D. 2021. Climate change may cause shifts in growth and instantaneous natural mortality of American shad throughout their native range. *Trans. Am. Fish. Soc.* **150**(3): 407–421. doi:10.1002/tafs.10299.
- Gresh, T., Lichatowich, J., and Schoonmaker, P. 2000. An estimation of historic and current levels of salmon production in the Northeast Pacific ecosystem: evidence of a nutrient deficit in the freshwater systems of the Pacific Northwest. *Fisheries*, **25**(1): 15–21. doi:10.1577/1548-8446(2000)025<0015:AEOHAC>2.0.CO;2.
- Gu, Z., Gu, L., Eils, R., Schlesner, M., and Brors, B. 2014. Circlize implements and enhances circular visualization in R. *Bioinformatics*, **30**: 2811–2812. doi:10.1093/bioinformatics/btu393.
- Guyette, M.Q., Loftin, C.S., Zydlewski, J., and Cunjak, R. 2014. Carcass analogues provide marine subsidies for macroinvertebrates and juvenile Atlantic salmon in temperate oligotrophic streams. *Freshw. Biol.* **59**(2): 392–406. doi:10.1111/fwb.12272.
- Haro, A. 2009. Challenges for diadromous fishes in a dynamic global environment. *American Fisheries Society*.
- Haskell, C.A. 2018. From salmon to shad: shifting sources of marine-derived nutrients in the Columbia River Basin. *Ecol. Freshw. Fish.* **27**(1): 310–322. doi:10.1111/eff.12348.
- Hicks, C.C., Cohen, P.J., Graham, N.A.J., Nash, K.L., Allison, E.H., D'Lima, C., et al. 2019. Harnessing global fisheries to tackle micronutrient deficiencies. *Nature*, **574**(7776): 95–98. doi:10.1038/s41586-019-1592-6.
- Hyder, K., Weltersbach, M.S., Armstrong, M., Ferter, K., Townhill, B., Ahvonen, A., et al. 2018. Recreational sea fishing in Europe in a global context — participation rates, fishing effort, expenditure, and implications for monitoring and assessment. *Fish. Fish.* **19**(2): 225–243. doi:10.1111/faf.12251.
- ICES. 2015. Report of the Workshop on Lampreys and Shads (WKLS), 27–29 November 2014, Lisbon, Portugal. ICES CM 2014/SSGEF:13.
- IUCN. 2020. The IUCN Red List of Threatened Species. Version 2020-3. Available from <https://www.iucnredlist.org>.
- Janetski, D.J., Chaloner, D.T., Tiegs, S.D., and Lamberti, G.A. 2009. Pacific salmon effects on stream ecosystems: a quantitative synthesis. *Oecologia*, **159**(3): 583–595. doi:10.1007/s00442-008-1249-x.
- Jatteau, P., Drouineau, H., Charles, K., Carry, L., Lange, F., and Lambert, P. 2017. Thermal tolerance of allis shad (*Alosa alosa*) embryos and larvae: modeling and potential applications. *Aquat. Living Resour.* **30**: 2. doi:10.1051/alr/2016033.
- Jolly, M.T., Arahamian, M.W., Hawkins, S.J., Henderson, P.A., Hillman, R., O'Maoiléidigh, N., et al. 2012. Population genetic structure of protected allis shad (*Alosa alosa*) and twaite shad (*Alosa fallax*). *Mar. Biol.* **159**(3): 675–687. doi:10.1007/s00227-011-1845-x.
- Joordens, J.C.A., Kuipers, R.S., Wanink, J.H., and Muskiet, F.A.J. 2014. A fish is not a fish: patterns in fatty acid composition of aquatic food may have had implications for hominin evolution. *J. Hum. Evol.* **77**: 107–116. doi:10.1016/j.jhevol.2014.04.004.
- Kielbassa, J., Delignette-Muller, M.L., Pont, D., and Charles, S. 2010. Application of a temperature-dependent von Bertalanffy growth model to bullhead (*Cottus gobio*). *Ecol. Modell.* **221**(20): 2475–2481. doi:10.1016/j.ecolmodel.2010.07.001.
- Kobayashi, M., Msangi, S., Batka, M., Vannuccini, S., Dey, M.M., and Anderson, J.L. 2015. Fish to 2030: the role and opportunity for aquaculture. *Aquacult. Econ. Manage.* **19**(3): 282–300. doi:10.1080/13657305.2015.994240.
- Kohler, A.E., Pearsons, T.N., Zendt, J.S., Mesa, M.G., Johnson, C.L., and Connolly, P.J. 2012. Nutrient enrichment with salmon carcass analogs in the Columbia River Basin, USA: a stream food web analysis. *Trans. Am. Fish. Soc.* **141**(3): 802–824. doi:10.1080/00028472.2012.676380.
- Kremen, C., Williams, N.M., Aizen, M.A., Gemmill-Herren, B., LeBuhn, G., Minckley, R., et al. 2007. Pollination and other ecosystem services produced by mobile organisms: a conceptual framework for the effects of land-use change. *Ecol. Lett.* **10**(4): 299–314. doi:10.1111/j.1461-0248.2007.01018.x.
- Lassalle, G., and Rochard, E. 2009. Impact of twenty-first century climate change on diadromous fish spread over Europe, North Africa and the Middle East. *Global Change Biol.* **15**(5): 1072–1089. doi:10.1111/j.1365-2486.2008.01794.x.
- Limburg, K.E., and Waldman, J.R. 2009. Dramatic declines in North Atlantic diadromous fishes. *BioScience*, **59**(11): 955–965. doi:10.1525/bio.2009.59.117.
- López-Hoffman, L., Varady, R.G., Flessa, K.W., and Balvanera, P. 2010. Ecosystem services across borders: a framework for transboundary conservation policy. *Front. Ecol. Environ.* **8**(2): 84–91. doi:10.1890/070216.
- MacAvoy, S.E., Macko, S.A., McIninch, S.P., and Garman, G.C. 2000. Marine nutrient contributions to freshwater apex predators. *Oecologia*, **122**(4): 0568. doi:10.1007/s004420050980.
- Martin, J., Rougemont, Q., Drouineau, H., Launey, S., Jatteau, P., Bareille, G., et al. 2015. Dispersal capacities of anadromous Allis shad population inferred from a coupled genetic and otolith approach. *Can. J. Fish. Aquat. Sci.* **72**(7): 991–1003. doi:10.1139/cjfas-2014-0510.
- McDowall, R.M. 1988. Diadromy in fishes: migrations between freshwater and marine environments. *Croom Helm*.
- Mennesson-Boisneau, C. 1990. Migration, répartition, reproduction et caractéristiques biologiques des aloses (*Alosa* sp.) dans le bassin de la Loire. Thèse de Doctorat, université de Rennes 1.
- Mennesson-Boisneau, C., Arahamian, M.W., Sabatié, M.R., and Cassou-Leins, J.J. 2000. Biologie des aloses: remontée migratoire des adultes. In *Les aloses (Alosa alosa et Alosa fallax spp.): écobiologie et variabilité des populations*. Edited by J. L. Baglinière and P. Elie. Cemagref, Inra Éditions, Paris. pp. 55–72.

- Millennium Ecosystem Assessment 2005. Ecosystems and human well-being: synthesis. Island Press, Washington, D.C.
- Mota, M. 2014. Biology and Ecology of Allis Shad, *Alosa alosa* (Linnaeus, 1758), in the Minho River. Ph.D. thesis, Porto University, Porto, Portugal.
- Mota, M., Rochard, E., and Antunes, C. 2016. Status of the diadromous fish of the Iberian Peninsula: past, present and trends. *Limnetica*, **35**: 1–18. doi:10.23818/limn.35.01.
- Naiman, R.J., Bilby, R.E., Schindler, D.E., and Helfield, J.M. 2002. Pacific salmon, nutrients, and the dynamics of freshwater and riparian ecosystems. *Ecosystems*, **5**(4): 399–417. doi:10.1007/s10021-001-0083-3.
- Olney, J.E., Latour, R.J., Watkins, B.E., and Clarke, D.G. 2006. Migratory behavior of American shad in the York River, Virginia, with implications for estimating in-river exploitation from tag recovery data. *Trans. Am. Fish. Soc.* **135**(4): 889–896. doi:10.1577/T05-101.1.
- Parmesan, C., and Yohe, G. 2003. A globally coherent fingerprint of climate change impacts across natural systems. *Nature*, **421**: 37–42. doi:10.1038/nature01286.
- Paumier, A., Drouineau, H., Carry, L., Nachón, D.J., and Lambert, P. 2019. A field-based definition of the thermal preference during spawning for allis shad populations (*Alosa alosa*). *Environ. Biol. Fishes*, **102**(6): 845–855. doi:10.1007/s10641-019-00874-7.
- Post, D.M., and Walters, A.W. 2009. Nutrient excretion rates of anadromous alewives during their spawning migration. *Trans. Am. Fish. Soc.* **138**(2): 264–268. doi:10.1577/T08-111.1.
- Randon, M., Daverat, F., Bareille, G., Jatteau, P., Martin, J., Pecheyran, C., and Drouineau, H. 2018. Quantifying exchanges of allis shads between river catchments by combining otolith microchemistry and abundance indices in a Bayesian model. *ICES J. Mar. Sci.* **75**(1): 9–21. doi:10.1093/icesjms/ifsx148.
- R Core Team 2018. R: a language and environment for statistical computing. R Foundation for Statistical Computing, Vienna, Austria. Available from <https://www.R-project.org>.
- Romero, E., Garnier, J., Lassaletta, L., Billen, G., Le Gendre, R., Riou, P., and Cugier, P. 2013. Large-scale patterns of river inputs in southwestern Europe: seasonal and interannual variations and potential eutrophication effects at the coastal zone. *Biogeochemistry*, **113**(1–3): 481–505. doi:10.1007/s10533-012-9778-0.
- Rosso, L., Lobry, J.R., Bajard, S., and Flandrois, J.P. 1995. Convenient model to describe the combined effects of temperature and pH on microbial growth. *Appl. Environ. Microbiol.* **61**(2): 610–616. doi:10.1128/aem.61.2.610-616.1995.
- Rougier, T. 2014. Repositionnement des poissons migrateurs amphihalins européens dans un contexte de changement climatique: une approche exploratoire par modélisation dynamique mécaniste. Ph.D. thesis, University of Bordeaux.
- Rougier, T., Drouineau, H., Dumoulin, N., Faure, T., Deffuant, G., Rochard, E., and Lambert, P. 2014. The GR3D model, a tool to explore the global repositioning dynamics of diadromous fish distribution. *Ecol. Modell.* **283**: 31–44. doi:10.1016/j.ecolmodel.2014.03.019.
- Rougier, T., Lassalle, G., Drouineau, H., Dumoulin, N., Faure, T., Deffuant, G., Rochard, E., and Lambert, P. 2015. The combined use of correlative and mechanistic species distribution models benefits low conservation status species. *PLoS ONE*, **10**(10): e0139194. doi:10.1371/journal.pone.0139194.
- Runge, C.A., Martin, T.G., Possingham, H.P., Willis, S.G., and Fuller, R.A. 2014. Conserving mobile species. *Front. Ecol. Environ.* **12**(7): 395–402. doi:10.1890/130237.
- Samways, K.M., Quiñones-Rivera, Z.J., Leavitt, P.R., and Cunjak, R.A. 2015. Spatiotemporal responses of algal, fungal, and bacterial biofilm communities in Atlantic rivers receiving marine-derived nutrient inputs. *Freshw. Sci.* **34**(3): 881–896. doi:10.1086/681723.
- Samways, K.M., Soto, D.X., and Cunjak, R.A. 2018. Aquatic food-web dynamics following incorporation of nutrients derived from Atlantic anadromous fishes: nutrients from anadromous fishes. *J. Fish Biol.* **92**(2): 399–419. doi:10.1111/jfb.13519.
- Scheuerell, M.D., Levin, P.S., Zabel, R.W., Williams, J.G., and Sanderson, B.L. 2005. A new perspective on the importance of marine-derived nutrients to threatened stocks of Pacific salmon (*Oncorhynchus* spp.). *Can. J. Fish. Aquat. Sci.* **62**(5): 961–964. doi:10.1139/f05-113.
- Schindler, D.E., Scheuerell, M.D., Moore, J.W., Gende, S.M., Francis, T.B., and Palen, W.J. 2003. Pacific salmon and the ecology of coastal ecosystems. *Front. Ecol. Environ.* **1**(1): 31–37. doi:10.1890/1540-9295(2003)001[0031:PSATEO]2.0.CO;2.
- Semmens, D.J., Diffendorfer, J.E., López-Hoffman, L., and Shapiro, C.D. 2011. Accounting for the ecosystem services of migratory species: quantifying migration support and spatial subsidies. *Ecol. Econ.* **70**(12): 2236–2242. doi:10.1016/j.ecolecon.2011.07.002.
- Semmens, D.J., Diffendorfer, J.E., Bagstad, K.J., Wiederholt, R., Oberhauser, K., Ries, L., et al. 2018. Quantifying ecosystem service flows at multiple scales across the range of a long-distance migratory species. *Ecosyst. Serv.* **31**: 255–264. doi:10.1016/j.ecoser.2017.12.002.
- Steffen, W., Broadgate, W., Deutsch, L., Gaffney, O., and Ludwig, C. 2015. The trajectory of the Anthropocene: the Great Acceleration. *Anthropocene Rev.* **2**(1): 81–98. doi:10.1177/2053019614564785.
- Stephens, P.A., Sutherland, W.J., and Freckleton, R.P. 1999. What is the Allee effect? *Oikos*, **87**(1): 185–190. doi:10.2307/3547011.
- Taverny, C. 1991. Contribution à la connaissance de la dynamique des populations d'aloses: *Alosa alosa* et *Alosa fallax* dans le système fluvio-estuarien de la Gironde: pêche, biologie et écologie. Étude particulière de la dévalaison et de l'impact des activités humaines. Doctorat Biologie des populations et écosystèmes, Université de Bordeaux I, 1991.
- Twining, C.W., Palkovacs, E.P., Friedman, M.A., Hasselman, D.J., and Post, D.M. 2017. Nutrient loading by anadromous fishes: species-specific contributions and the effects of diversity. *Can. J. Fish. Aquat. Sci.* **74**(4): 609–619. doi:10.1139/cjfas-2016-0136.
- von Bertalanffy, L. 1938. A quantitative theory of organic growth (inquiries on growth laws. II). *Hum. Biol.* **10**(2): 181–213.
- Walters, A.W., Barnes, R.T., and Post, D.M. 2009. Anadromous alewives (*Alosa pseudoharengus*) contribute marine-derived nutrients to coastal stream food webs. *Can. J. Fish. Aquat. Sci.* **66**(3): 439–448. doi:10.1139/F09-008.
- Weaver, D.M., Coghlan, S.M., and Zydlewski, J. 2018. Effects of sea lamprey substrate modification and carcass nutrients on macroinvertebrate assemblages in a small Atlantic coastal stream. *J. Freshw. Ecol.* **33**(1): 19–30. doi:10.1080/02705060.2017.1417168.
- Weber, M.J., and Brown, M.L. 2018. Effects of resource pulse magnitude on nutrient availability, productivity, stability, and food web dynamics in experimental aquatic ecosystems. *Hydrobiologia*, **814**(1): 191–203. doi:10.1007/s10750-018-3536-9.
- West, D.C., Walters, A.W., Gephard, S., and Post, D.M. 2010. Nutrient loading by anadromous alewife (*Alosa pseudoharengus*): contemporary patterns and predictions for restoration efforts. *Can. J. Fish. Aquat. Sci.* **67**(8): 1211–1220. doi:10.1139/F10-059.
- Wilson, K., and Veneranta, L. (Editors). 2019. Data-limited diadromous species? Review of European status. ICES. doi:10.17895/ICES.PUB.5253.
- Wipfli, M.S., Hudson, J.P., Caouette, J.P., and Chaloner, D.T. 2003. Marine subsidies in freshwater ecosystems: salmon carcasses increase the growth rates of stream-resident salmonids. *Trans. Am. Fish. Soc.* **132**(2): 371–381. doi:10.1577/1548-8659(2003)132<0371:MSIFES>2.0.CO;2.

## Appendix A. Detailed description of the GR3D model and its physical environment

### Overall model description

GR3D (Global Repositioning Dynamics for Diadromous fish Distribution) was developed to assess the repositioning of diadromous species under climate change over large spatial and temporal scales. It was written in Java using the “SimAqualife” software framework especially designed for spatialized and individual-based simulations of aquatic life movements. GR3D is an individual-based stochastic model. It integrates and combines population dynamics with explicit formulation of key life-history processes and climatic requirements.

GR3D was developed to cover the entire life cycle of any diadromous fish species. The model was divided into six sub-models consistent with the life cycle events and processes of any diadromous species (i.e., reproduction, growth, survival, downstream migration, maturation, dispersal and upstream migration). A set of 42 parameters is associated to the different processes with parameter values obtained either from literature, expert elicitation or calibration (Table A1). The model was first parameterized for allis shad (*Alosa alosa*) in western Europe.

### Population dynamics within the model

Individuals reproduce every spring in a river basin and produce juveniles. The number of recruits  $R_j$  produced by the spawning stock  $S_j$  in a given basin  $j$  is assumed to follow a Beverton–Holt stock–recruitment relationship of parameters  $\alpha_j$  and  $\beta_j$  (BH-SR; eq. A1).

The recruitment  $r_0$  is linked to species fecundity ( $\alpha$ ) and depends on the number of spawners  $S_j$  in the spawning basin  $j$ . The BH-SR included in GR3D differs from the traditional BH-SR in two aspects:

- (1) An “Allee effect” is included within the reproductive process to simulate difficulties to settle a functional population with limited numbers of individuals in new habitats. Depensation strength (i.e., the number of spawners that effectively participate in reproduction) is depending on the river basin surface ( $w_a$ ) through the  $\eta$  and  $\theta$  parameters. The intensity of the “Allee effect” is positively correlated to parameter  $\eta$  and negatively correlated to parameter  $\theta$ .
- (2) The mortality from eggs to recruits is modeled as a function of temperature and spawning basin surface. The non-density-

**Table A1.** Description of the GR3D parameters with nominal values for the 42 parameters included in the model.

Parameter name	Description	Nominal value
<b>Reproduction</b>		
repSeason	Season of the reproduction	Spring
$\Delta t_{rec}$	Assumed age of juvenile produced by the reproduction (years)	0.33
$\eta$	Parameter to relate $S_{95,j}$ and the surface of a spawning place (individuals·km <sup>-2</sup> )	2.4
$\theta$	Ratio between $S_{95,j}$ and $S_{50,j}$ in each spawning place	1.9
$\alpha^*$	Fecundity of the species (eggs·individual <sup>-1</sup> )	270 000
surv <sub>OptRep</sub>	Optimal survival rate of an individual from eggs to the age $\Delta t_{rec}$	$1 \times 7^{-3}$
$T_{minRep}, T_{OptRep}, T_{maxRep}$	Water temperature (°C) regulating survival of an individual from eggs to the age $\Delta t_{rec}$	(9.3, 20.8, 31) <sup>a</sup>
$\lambda$	Parameter to relate $c_j$ and the surface of a spawning place	$4.1 \times 10^{-4}$
$\sigma_{rep}$	Standard deviation of log-normal distribution of the recruitment	0.2
Sp <sub>sp</sub>	Survival probability of spawners after reproduction	0.1
<b>Downstream migration</b>		
downMigAge	Age of individual when it runs toward the sea (years)	0.33
downMigSeason	Season of the run toward the sea	Summer
<b>Growth</b>		
$L_{inf}$	Initial length of juveniles in estuary (cm)	2
$\sigma_{\Delta L}$	Standard deviation of log-normal distribution of the growth increment	0.2
$L_{\infty}^*$	Asymptotic length of an individual (cm)	70 <sup>b</sup>
$T_{minGrow}, T_{optGrow}, T_{maxGrow}$	Water temperature (°C) regulating the growth	(3, 17, 26)
$k_{optGrowFemale}^*$	Optimal growth coefficient for females and males (cm·season <sup>-1</sup> )	0.3236 <sup>b</sup>
$k_{optGrowMale}^*$		0.2141 <sup>b</sup>
<b>Survival</b>		
$Z_{sea}$	Annual mortality coefficient at sea (year <sup>-1</sup> )	0.4
$H_{riv}$	Annual mortality (different from natural) coefficient in river (year <sup>-1</sup> )	0
$T_{minSurvRiv}, T_{optSurvRiv}, T_{maxSurvRiv}$	Water temperature (°C) regulating survival of individuals in river	(10.7, 17, 25.7) <sup>c</sup>
surv <sub>OptRiv</sub>	Optimal natural survival rate of individuals in river (year <sup>-1</sup> )	1
<b>Maturation</b>		
$L_{matFemale}^*$	Length at first maturity (cm)	55 <sup>b</sup>
$L_{matMale}^*$		40 <sup>b</sup>
<b>Upstream migration</b>		
upMigAge	Age of an individual when it runs toward the river (years)	—
upMigSeason	Season of the return of spawners in river for spawning	Spring
$p_{hom}$	Probability to do natal homing behavior	0.75
$\alpha_{const}, \alpha_{dist}, \alpha_{TL}, \alpha_{WA}$	Parameters of the logit function used to determine the weight of each accessible basin for dispersers–strays	-2.9, 19.7, 0, 0
$D_{j-birthPlace}, \sigma_{j-birthPlace}, TL, \sigma_{TL}, \overline{WA}, \sigma_{WA}$	Mean and standard deviation used for standard core values in the logit function	300, 978, —, —, —, —
$w_{deathBasin}$	Weight of the death basin used to introduce a mortality of dispersers–strays	(0.2–0.6)

**Note:** An asterisk marked parameters modified from the original GR3D version (Rougier et al. 2014). New parameters values were obtained from either literature or offline calibration.

<sup>a</sup>Modified from Jatteau et al. (2017).

<sup>b</sup>Computed from offline calibration.

<sup>c</sup>Modified from Paumier et al. (2019).

dependent mortality is a function of temperature ( $\alpha_j$  and  $\beta_j$ ). The relationship between the non-density mortality and the water temperature follows a dome-shaped curve. Thus,  $T_{minR}$  and  $T_{maxR}$  define the range in which temperature ensures recruitment and egg survival, with an optimal survival at  $T_{optR}$ . The density-dependent mortality of the BH-SR depends on basin surface (through a population parameter  $\lambda$ ) to consider resource limitations in small basins.

$$(A1) \quad R_j = \frac{\alpha_j S_j \left\{ \frac{1}{1 + e^{\left[ \frac{-\ln(19) S_j - (\eta/\theta) W A_j}{\eta W A_j - (\eta/\theta) W A_j} \right]}} \right\}}{\beta_j + S_j \left\{ \frac{1}{1 + e^{\left[ \frac{-\ln(19) S_j - (\eta/\theta) W A_j}{\eta W A_j - (\eta/\theta) W A_j} \right]}} \right\}}$$

After the reproduction, the probability of spawners to survive is given through the  $Sp_{sp}$  parameter. For semelparous species dying after reproduction, this probability is set to a low value of 0.1.

Growth of individuals is modeled as a von Bertalanffy growth function. An effect of water temperature ( $T$ , °C) on the growth coefficient  $k$  is introduced in the process through a dome-shaped relationship as it was described above for reproduction (eq. A2). Thus, at  $T_{optGrow}$ , the growth coefficient is optimum ( $k_{optGrow}$ ) and becomes null when  $T$  is out of the range defined by  $T_{minGrow}$  and  $T_{maxGrow}$ :

$$(A2) \quad k = k_{optGrow} \frac{(T - T_{minGrow})(T - T_{maxGrow})}{(T - T_{minGrow})(T - T_{maxGrow})(T - T_{optGrow})}$$

After spending several years at sea, ripe individuals (here an individual is assumed to be mature when it reaches its size at

**Fig. A1.** Map of the 135 European river basins implemented into the GR3D physical environment. The 13 rivers basins used for model partial validation are represented in dark grey. Sources: European Commission (2007) and Lehner et al. (2008). Projection: WGS 84.



maturity,  $L_{mat}$ ) start their spawning migration and enter a river basin to reproduce. The upstream migration included an original dispersal process that is designed as a three-stage process with (1) emigration, (2) transfer, and (3) settlement phases.

1. During the emigration phase, individuals have a probability to adopt a homing behavior ( $p_{hom}$ ) or a straying behavior ( $1 - p_{hom}$ ), with  $p_{hom}$  defined as a model parameter.
2. During the transfer phase, individuals that do not adopt a straying behavior, simply migrate to their natal river. For strayers, the probability to migrate in each river basin is assumed to be a function of its accessibility. Accessibility is assumed to depend on dispersal distance between the natal basin and the new basin  $j$ . Then, relatively to an individual, a weight is calculated for each river basin using a logit function with some parameters defined as model parameters. Assuming that the individuals may not find a basin and simply die during transfer, a virtual “death basin” with a fixed weight ( $w^{deathBasin}$ ) is also introduced. The probability to choose each river basin (including the death one) was obtained by standardizing all the weights so that their sum equals 1. The choice of a destination basin is then modeled by a simple multinomial process.
3. During the settlement phase, individuals enter in the destination basin, survive if conditions are suitable and reproduce if they find mating requirements.

The dispersal was then modeled by eq. A3:

$$(A3) \quad w_{j_1 \rightarrow j_2} = \frac{1}{1 + e^{\alpha_0 + \alpha_1 \frac{(D_{j_1 \rightarrow j_2} - \mu_D)}{\sigma_D}}}$$

where  $D_{j_1 \rightarrow j_2}$  is the distance between the departure and destination basins,  $\alpha_0$  and  $\alpha_1$  are the kernel parameters, and  $\mu_D$  and  $\sigma_D$  are the mean and standard deviation for the inter-basin distances.

At each time step, the probability of each individual to survive is estimated regarding its location along the land–sea continuum. The seasonal survival probability ( $Sp_{sea}$ ) is based on the annual mortality coefficients  $Z_{sea}$  and  $H_{river}$ , which depend on age and water temperature.

### Description of the physical environment

The physical environment of the model is composed of a set of both river and sea basins connected to each other and spatially geo-referenced. Both river and sea basins are characterized by seasonal temperature time series ( $T$ , °C), while river basins are also characterized by their surface ( $km^2$ ). The physical environment included 135 river basins along the European Atlantic coast, ranging from the south of Portugal to the British Isles and Norway (Fig. A1).

### Description of the data used to compare model estimates and observations of allis shad abundances in the 13 well-studied rivers

Data regarding allis shad spawner abundance were derived from several sources.

For the Lima, Minho, and Adour rivers, abundances were estimated from annual commercial fishery landings (e.g., Mota et al. 2015).

For the Lima and Adour rivers, landings were given in kilograms of fish caught, so biomass was divided by an average mass of fish;  $W = 2.1$  kg in the Lima and  $W = 1.7$  kg in the Adour, respectively (ICES 2015), to broadly estimate fish abundances in both rivers.

For the Garonne and the Charente rivers, abundances were derived from the counting of spawning events. During the reproduction, shads exhibit a circular and noisy movement, hereinafter called “splash” at the water surface, that can be recorded to monitor the spawning activity (Mennesson-Boisneau 1990). The number of “splashes” recorded is often used as a good estimator to assess the spawning stock.

For the other rivers, a video-counting system at fishways was used to assess the spawning stock. Video-counting provide reliable estimates of migrating adults, because systems are usually located downstream of the main spawning grounds but some fish may not cross the barriers and therefore are not counted by the device (P. Jatteau, personal observation).

For several rivers, data do not discriminate between *A. fallax* and *A. alosa* and provide a net annual balance between adults migrating upstream and juveniles migrating downstream.

## References

- European Commission. 2007. Joint Research Centre. Institute for Environment and Sustainability. A pan-European river and catchment database. Publications Office, LU. Available from <https://data.europa.eu/doi/10.2788/35907>.
- ICES. 2015. Report of the Workshop on Lampreys and Shads (WKLS), 27–29 November 2014, Lisbon, Portugal. ICES CM 2014/SSGEF:13.
- Jatteau, P., Drouineau, H., Charles, K., Carry, L., Lange, F., and Lambert, P. 2017. Thermal tolerance of allis shad (*Alosa alosa*) embryos and larvae: Modeling and potential applications. *Aquat. Living Resour.* **30**: 2. doi:10.1051/alr/2016033.
- Lehner, B., Verdin, K.L., and Jarvis, A. 2008. New global hydrography derived from spaceborne elevation data. *Eos*, **89**: 93–94. doi:10.1029/2008EO100001.
- Mennesson-Boisneau, C. 1990. Migration, répartition, reproduction et caractéristiques biologiques des aloses (*Alosa* sp.) dans le bassin de la Loire.
- Mota, M., Bio, A., Bao, M., Pascual, S., Rochard, E., and Antunes, C. 2015. New insights into biology and ecology of the Minho River Allis shad (*Alosa alosa* L.): contribution to the conservation of one of the last European shad populations. *Rev. Fish Biol. Fish.* **25**(2): 395–412. doi:10.1007/s11160-015-9383-0.
- Paumier, A., Drouineau, H., Carry, L., Nachón, D.J., and Lambert, P. 2019. A field-based definition of the thermal preference during spawning for allis shad populations (*Alosa alosa*). *Environ. Biol. Fishes*, **102**(6): 845–855. doi:10.1007/s10641-019-00874-7.
- Rougier, T., Drouineau, H., Dumoulin, N., Faure, T., Deffuant, G., Rochard, E., and Lambert, P. 2014. The GR3D model, a tool to explore the global repositioning dynamics of diadromous fish distribution. *Ecol. Model.* **283**: 31–44. doi:10.1016/j.ecolmodel.2014.03.019.